The 16th Cambridge Workshop on Cool Stars, Stellar Systems and the Sun
ASP Conference Series, Vol. 448
Christopher M. Johns-Krull, Matthew K. Browning, and Andrew A. West, eds.

The Mouse that Roared: A SuperFlare from the dMe Flare Star EV Lac Detected by Swift and Konus-Wind

Rachel A. Osten,[1] Olivier Godet,[2] Stephen Drake,[3] Jack Tueller,[3] Jay Cummings,[3] Hans Krimm,[3] John Pye,[4] Valentin Pal'shin,[5] Sergei Golenetskii,[5] Fabio Reale,[6] Samantha R. Oates,[7] Mat J. Page,[7] and Andrea Melandri[8]

[1]*Space Telescope Science Institute 3700 San Martin Drive, Baltimore, MD 21218 USA*

[2]*Université de Toulouse, UPS, CESR, 9 avenue du Colonel Roche, 31028 Toulouse Cedex 9, France*

[3]*NASA Goddard Space Flight Center, Greenbelt MD USA*

[4]*Department of Physics and Astronomy, University of Leicester, University Road, Leicester LE1 7RH UK*

[5]*Ioffe Physico-Technical Institute, Laboratory for Experimental Astrophysics , 26 Polytekhnicheskaya, St Petersburg 194021, Russian Federation*

[6] *Dip. Scienze Fis. & Astron., Sez. Astron.,Universitá di Palermo,P.za Parlamento 1, 90134 Palermo, Italy*

[7] *Mullard Space Science Laboratory, University College London, Holmbury St. Mary, Dorking, Surrey, RH5 6NT, UK*

[8] *Astrophysics Research Institute, Liverpool John Moores University, Twelve Quays House, Birkenhead CH41 1LD UK*

Abstract. We report on a large stellar flare from the nearby dMe flare star EV Lac observed by the Swift and Konus-Wind satellites and the Liverpool Telescope. It is the first large stellar flare from a dMe flare star to result in a Swift trigger based on its hard X-ray intensity. Its peak f_X from 0.3–100 keV of 5.3×10^{-8} erg cm^{-2} s^{-1} is nearly 7000 times larger than the star's quiescent coronal flux, and the change in magnitude in the white filter is ≥4.7. This flare also caused a transient increase in EV Lac's bolometric luminosity (L_{bol}) during the early stages of the flare, with a peak estimated L_X/L_{bol} ~3.1. We apply flare loop hydrodynamic modeling to the plasma parameter temporal changes to derive a loop semi-length of $l/R_\star = 0.37\pm0.07$. The soft X-ray spectrum of the flare reveals evidence of iron Kα emission at 6.4 keV. We model the Kα emission as fluorescence from the hot flare source irradiating the photospheric iron, and derive loop heights of $h/R_\star$=0.1, consistent within factors of a few with the heights inferred from hydrodynamic modeling. The Kα emission feature shows variability on time scales of ~200 s which is difficult to interpret using the pure fluorescence hypothesis. We examine Kα emission produced by collisional ionization from accelerated particles, and find parameter values for the spectrum of accelerated particles which can accommodate the increased amount of Kα flux and the lack of observed nonthermal emission in the 20-50 keV spectral region.

1. Introduction

EV Lac has a record of frequent (Huenemoerder et al. 2009) and large outbursts, from optical flaring (Kodaira et al. 1976; Roizman & Shevchenko 1982) to radio (Osten et al. 2005) to X-ray (Schmitt 1994; Favata et al. 2000) wavelengths. On April 25, 2008, EV Lac underwent an outburst which was serendipitously detected by two Gamma-Ray Burst satellites and had supporting ground-based observations. This flare was detected by its transient *hard X-ray* flux, belonging to a small handful of stellar flares which have been triggered using this method. These results have been published in Osten et al. (2010); we provide highlights of the results in this conference proceedings.

2. Light Curves

With the exception of the Konus data, there is no information on the flux variation of EV Lac prior to the trigger by the Burst Alert Telescope (BAT). The trigger time was 2008 April 25 T05:13:57. Figure 1 displays the temporal behavior of the flare as it was caught by the different satellites/instruments involved. The left panel details evolution over the first ∼hour, while the right panel details evolution on longer timescales, up to 40,000 s after the trigger. The Konus data indicate that the peak of the flare was achieved within a minute of the source entering the BAT field of view and causing the trigger. The following instruments/telescopes recorded information on the flare: Konus/Wind, Swift/BAT, Swift/X-ray Telescope (XRT), Swift/UV Optical Telescope (UVOT), and Liverpool Telescope (LT).

The blue horizontal lines in Figure 1 indicate the times over which X-ray spectra were extracted. Because of the high count rates, annular regions in the wings of the PSF had to be used to avoid pile-up. Sparse photometric coverage was obtained, indicated in the bottom panel (v); the flare seen in the white filter was brighter than the count rate limit for the UV Optical Telescope, causing a safing event; thus only a lower limit is obtained. Nevertheless, this allows a lower limit on the optical area involved, under the assumption that the white light flare can be described by a black-body with temperature near 10^4K.

3. Time Variation of Plasma Parameters and Spectral Modelling

Time-resolved spectroscopy was performed on data from the XRT and BAT, with different time intervals. The blue horizontal lines in Figure 1 indicate the times when spectra were extracted. APEC model fits were performed to the X-ray spectra. For BAT spectra in the 14-100 keV range, a single temperature only was needed, while for the XRT spectra in the 0.3-10 keV range, two temperatures were used. The variation of temperature and volume emission measure (VEM) with time is smooth, and there are no apparent abundance (Z) variations. In the early stages of the flare, the X-ray luminosity exceeds the bolometric luminosity, by a factor of ∼3 at the largest. The right figure shows a fit to both the XRT and BAT spectra over the time interval T0+171 s:T0+961 s. Two temperatures are adequate to fit both soft and hard X-ray emission; no additional thermal or nonthermal component is needed.

By using Reale et al. (1997)'s hydrodynamic modelling method applied to Swift data, we can estimate the coronal loop length during the decay phase as:

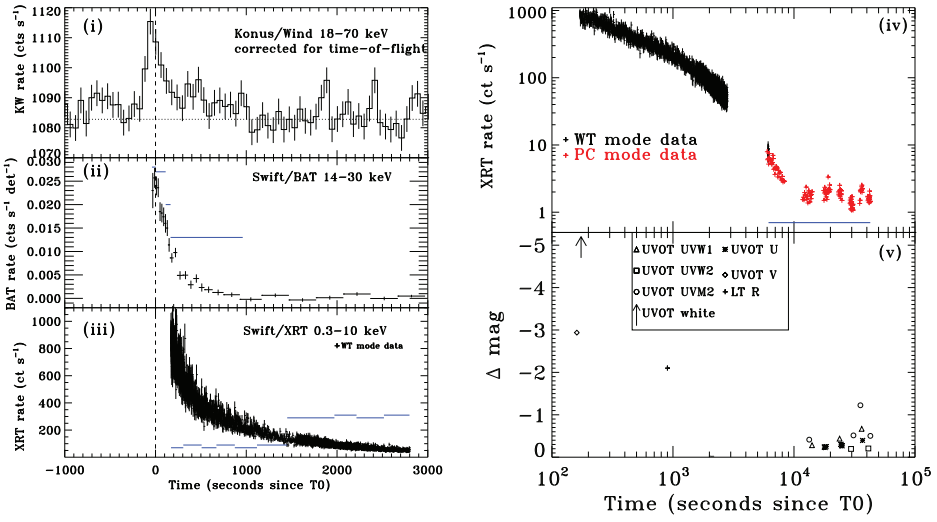

Figure 1. Left panel shows light curves in the initial stages of the flare decay of EV Lac, right panel shows light curves at later times.

$$L = \frac{\tau_{lc}\sqrt{(T)}}{\alpha F(\zeta)} \tag{1}$$

where τ_{lc} is the light curve exponential decay time, T is the flare maximum temperature, related to the maximum best-fit temperature through calibration of this method to the instrument under consideration, α=3.7×10^{-4} cm^{-1} s^{-1} K$^{1/2}$, and $F(\zeta)$ is a function which quantifies the amount of heating occurring during the decay phase of the flare. The variable ζ is the slope in the log(density-temperature) plane, or equivalently, 0.5*log(VEM)-log(T) plane. The result is l/R$_\star$=0.37±0.07, or for a vertical semi-circular loop, h/R$_\star$=0.24±0.04.

4. Kα Emission

One of the most surprising findings of this investigation was the clear detection of the Iron Kα emission line at 6.4 keV in the initial stages of the flare decay. Figure 2 shows a close-up of a spectrum in the 5–8 keV region detailing this. When fitting the data with only APEC plasma components, there is a clear excess around 6.4 keV which we attribute to emission from the Iron Kα line. Besides the Sun, there are only two other cool stars which have shown evidence for this feature during large stellar flares: the active binary system II Peg (Osten et al. 2007), and the single active evolved star HR 9024 (Testa et al. 2008). The line, at 6.4 keV, is formed from neutral or nearly neutral iron after a K shell electron is removed. The conventional mechanism as to what causes this is photoionization by X-rays above the photoionization edge of 7.11 keV. In the stellar context, it is cold iron which produces the emission, but the source of the radiation is the high energy photons from coronal plasma. Thus, in one X-ray spectrum, information about both coronal and photospheric material is obtained. The utility of

the emission line as a diagnostic in the stellar context stems from the dependence of the line strength on the height of the coronal (X-ray-emitting) material above the neutral (photospheric) material. Drake et al. (2008) have explored the emission strength of Iron Kα as a function of height for different scenarios, and we use their results to interpret our line strengths. The luminosity above 7.11 keV is required, as is the fluorescent efficiency, which depends on both the plasma temperature and the height of the X-ray source above the fluorescent source. The interpretation is done self-consistently for each time interval, using the results of the spectral modelling for that time interval. The source heights are in general agreement with the one derived using the hydrodynamic modelling from investigation of the plasma parameters, and indicates a fairly compact loop, with $h/R_\star \lesssim 0.3$.

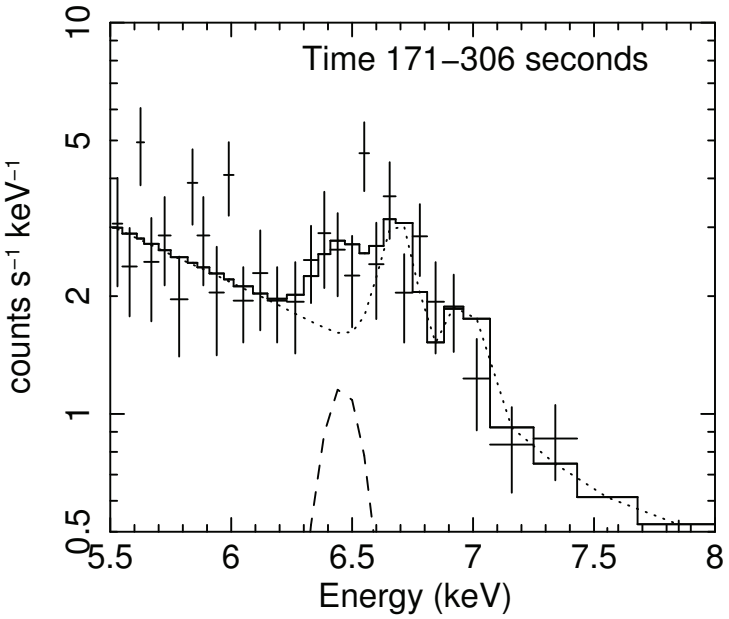

Figure 2. X-ray spectrum of EV Lac during the time period listed. The times refer to seconds since the BAT trigger time. The pluses indicate data and errors, the histogram is the fit to the data including all model components. The dotted line shows the thermal plasma components, while the dashed line shows the Gaussian component at 6.4 keV.

5. Kα Variability

Because there were a large number of time intervals in the initial decay of the flare, we explored the intensity of the Kα emission line in each of the time intervals. Table 1 lists the emission line parameters derived for the first ten time intervals. We only considered time intervals in which the probability was more than 97%. This results in five time intervals in the beginning stages of the flare decay having Iron Kα detections, but with variability detected on quite short timescales: in the time interval T0+306:T0+508, the line is not detected, and then in the next time interval, T0+508:T0+671, the line is detected with a strength much larger than what would be predicted for a fluorescent

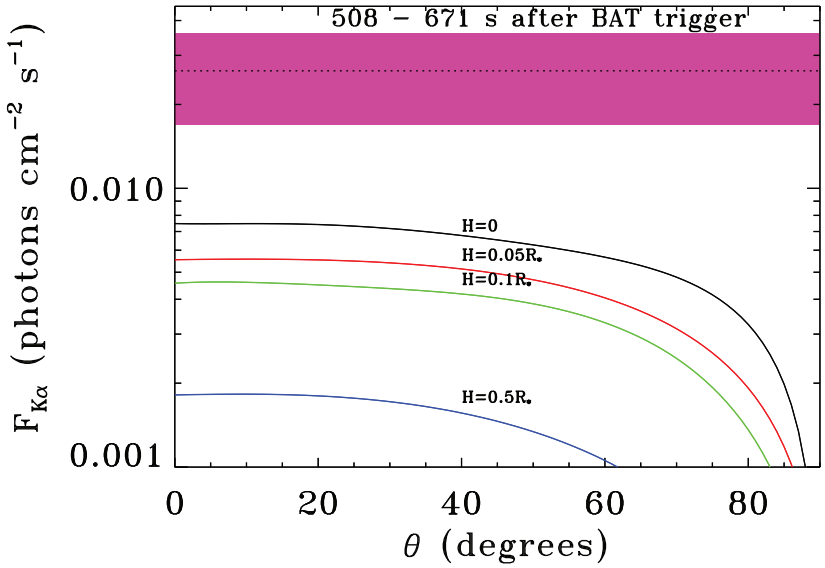

Figure 3. Modelling of the time interval 508–671 s after the BAT trigger, when the Iron Kα line showed an increase in line strength compared with time intervals near it. The dotted line shows the measured value of the line strength, and the magenta curve shows the 3σ error range. The curves below indicate the expected value of the Kα flux for different heights of the X-ray emitting source above the photosphere. Even for the most compact source, the observed flux cannot be reproduced with a purely fluorescent process.

Table 1. Iron Kα Emission Line Parameters

Time Interval (s)	E_0^1 (keV)	EW[2] (eV)	F[3] (10^{-3} photons cm^{-2} s^{-1})	P[4]
T0+171:T0+306	6.44 ± 0.08	$146^{+67}_{-72.5}$	$27.3^{+14.7}_{-12.9}$	99.94
T0+306:T0+508	$6.42^{+0.31}_{-0.41}$	$52.2^{+64.8}_{-52.2}$	$6.96^{+8.23}_{-6.96}$	55.42
T0+508:T0+671	6.41 ± 0.04	320 ± 102	$26.4^{+9.6}_{-9.5}$	99.97
T0+671:T0+874	$6.42^{+0.07}_{-0.10}$	103^{+95}_{-81}	$6.51^{+4.67}_{-4.37}$	99.19
T0+874:T0+1118	$6.46^{+0.05}_{-0.06}$	143^{+106}_{-114}	$6.86^{+4.18}_{-4.04}$	99.92
T0+1118:T0+1451	$6.41^{+0.15}_{-0.41}$	$84.3^{+155.7}_{-84.3}$	$2.65^{+2.35}_{-2.33}$	97.69
T0+1451:T0+1971	$6.45^{+0.10}_{-0.09}$	91^{+139}_{-91}	$2.12^{+2.02}_{-1.63}$	. . .
T0+1971:T0+2215	$6.38^{+0.11}_{-0.12}$	$94.8^{+288.2}_{-94.8}$	$1.20^{+0.94}_{-1.06}$	. . .
T0+2215:T0+2517	$6.11^{+0.20}_{-0.11}$	$331^{+52}_{-281.3}$	1.65 ± 0.85	. . .
T0+2517:T0+2798	$6.22^{+0.13}_{-0.22}$	295^{+302}_{-295}	$0.95^{+0.77}_{-0.71}$	. . .

[1] center of Gaussian fitted to data
[2] equivalent width of emission line
[3] flux in emission line
[4] probability from Monte Carlo simulations for significance of detection

process using the plasma parameters. Figure 3 shows the observed line strength as a function of astrocentric angle θ (defined so that $\theta = 0$ is on the center of the stellar disk and $\theta = 90$ is on the limb). Also plotted are the expected values of the line strength for different heights of the X-ray emitting source above the photosphere. Even for the most compact X-ray source, the Iron Kα emission is too strong to be explained by a purely fluorescence mechanism.

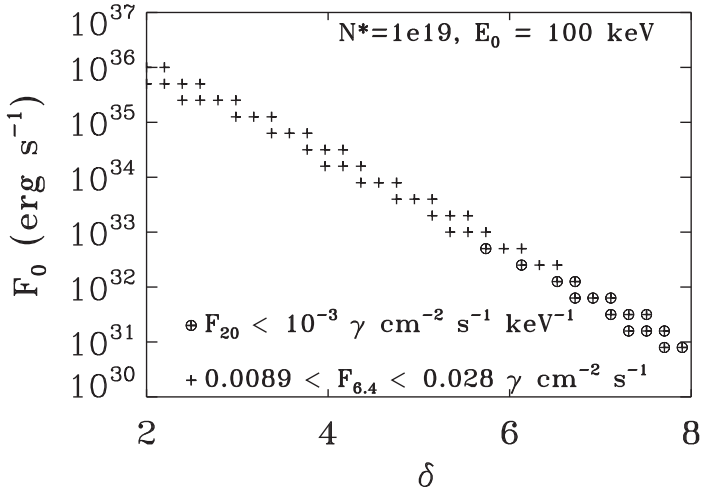

Figure 4. Parameters describing accelerated electrons within the context of explaining the enhanced level of Kα line flux. Pluses indicate values of total power and index δ which can produce the excess Kα emission seen, while pluses with circles around them satisfy the additional constraint that the nonthermal bremmstrahlung radiation at 20 keV is less than 10^{-3} photons cm^{-2} s^{-1} keV^{-1}.

Motivated by a few solar studies that showed flares which had excess Iron Kα line strengths above that which could be predicted from fluorescence mechanisms, we explored the addition of another Kα-producing mechanism. Figure 4 shows our attempt to interpret the excess Kα emission observed from T0+508 s: T0+671 s as collisional ionization from accelerated electrons. This is based upon the observation of excess Kα emission in a few solar flares above that accounted for by fluorescence (Emslie et al. 1986; Zarro et al. 1992). We use two constraints: the spectrum and amount of accelerated electrons must be enough to produce the excess Kα emission, but produce a nonthermal bremsstrahlung flux below the hard X-ray photon flux level observed (10^{-3} photons cm^{-2} s^{-1} keV^{-1} at 20 keV). Parameter values with encircled pluses fit this constraint. With this interpretation, and the lower limit on photospheric flare area of 2×10^{19} cm^2, we can estimate the nonthermal beam flux of 10^{11}-10^{14} erg cm^{-2} s^{-1}, which overlaps the range seen and modeled in solar and stellar flares, respectively (Allred et al. 2005, 2006).

6. Conclusions

The flare studied in this paper is unique in two main aspects: the level of X-ray radiation marks it as one of the most extreme flares yet observed in terms of the enhancement

of ∼7000 compared to the usual emission levels, and it is one of only a handful of stellar flares from normal stars without disks to exhibit the Fe Kα line, with a maximum equivalent width of >200 eV.

References

Allred, J. C., Hawley, S. L., Abbett, W. P., & Carlsson, M. 2005, ApJ, 630, 573. arXiv:astro-ph/0507335
— 2006, ApJ, 644, 484. arXiv:astro-ph/0603195
Drake, J. J., Ercolano, B., & Swartz, D. A. 2008, ApJ, 678, 385. 0710.0621
Emslie, A. G., Phillips, K. J. H., & Dennis, B. R. 1986, Solar Phys., 103, 89
Favata, F., Reale, F., Micela, G., Sciortino, S., Maggio, A., & Matsumoto, H. 2000, A&A, 353, 987. arXiv:astro-ph/9909491
Kodaira, K., Ichimura, K., & Nishimura, S. 1976, PASJ, 28, 665
Osten, R. A., Drake, S., Tueller, J., Cummings, J., Perri, M., Moretti, A., & Covino, S. 2007, ApJ, 654, 1052. arXiv:astro-ph/0609205
Osten, R. A., Godet, O., Drake, S., Tueller, J., Cummings, J., Krimm, H., Pye, J., Pal'shin, V., Golenetskii, S., Reale, F., Oates, S. R., Page, M. J., & Melandri, A. 2010, ApJ, 721, 785. 1007.5300
Osten, R. A., Hawley, S. L., Allred, J. C., Johns-Krull, C. M., & Roark, C. 2005, ApJ, 621, 398. arXiv:astro-ph/0411236
Reale, F., Betta, R., Peres, G., Serio, S., & McTiernan, J. 1997, A&A, 325, 782
Roizman, G. S., & Shevchenko, V. S. 1982, Soviet Astronomy Letters, 8, 85
Schmitt, J. H. M. M. 1994, ApJS, 90, 735
Testa, P., Drake, J. J., Ercolano, B., Reale, F., Huenemoerder, D. P., Affer, L., Micela, G., & Garcia-Alvarez, D. 2008, ApJ, 675, L97. 0801.3857
Zarro, D. M., Dennis, B. R., & Slater, G. L. 1992, ApJ, 391, 865